

# Magnetic coupling in $\text{CoCr}_2\text{O}_4$ and $\text{MnCr}_2\text{O}_4$ : an LSDA+ $U$ study

Claude Ederer

Department of Physics, Columbia University, 538 West 120th Street, New York, NY 10027, U.S.A.\*

Matej Komelj

Jožef Stefan Institute, Jamova 39, SI-1000 Ljubljana, Slovenia

(Dated: July 4, 2021)

We present a first principles LSDA+ $U$  study of the magnetic coupling constants in the spinel magnets  $\text{CoCr}_2\text{O}_4$  and  $\text{MnCr}_2\text{O}_4$ . Our calculated coupling constants highlight the possible importance of  $AA$  interactions in spinel systems with magnetic ions on both  $A$  and  $B$  sites. Furthermore, we show that a careful analysis of the dependence of the magnetic coupling constants on the LSDA+ $U$  parameters provides valuable insights in the underlying coupling mechanisms, and allows to obtain a quantitative estimate of the magnetic coupling constants. We discuss in detail the capabilities and possible pitfalls of the LSDA+ $U$  method in determining magnetic coupling constants in complex transition metal oxides.

## I. INTRODUCTION

Geometrically frustrated spin systems exhibit a low-temperature behavior that is fundamentally different from conventional (non-frustrated) spin systems.<sup>1,2</sup> The incompatibility between local interactions and global symmetry in geometrically frustrated magnets leads to a macroscopic degeneracy that prevents these systems from ordering. In some cases this degeneracy is lifted by further neighbor interactions or by a symmetry-breaking lattice distortion, resulting in ordered spin structures at temperatures that are significantly lower than what would be expected simply from the strength of the nearest neighbor interaction. Since usually several different ordered configurations with comparable energy exist in these systems, a very rich low temperature phase diagram can be observed.

Recently, it has been found in various magnetic spinel systems (general chemical formula:  $AB_2X_4$ ) that the geometrical frustration among the  $B$  sites in the spinel structure can give rise to pronounced effects due to *spin-lattice coupling*. In  $\text{ZnCr}_2\text{O}_4$  and  $\text{CdCr}_2\text{O}_4$  the macroscopic degeneracy is lifted by a tetragonal lattice distortion, resulting in complicated non-collinear spin ordering.<sup>3,4</sup> In addition, a pronounced splitting of certain phonon modes due to strong *spin-phonon coupling* has been found in  $\text{ZnCr}_2\text{O}_4$ .<sup>5,6</sup> Non-collinear spiral magnetic ordering at low temperatures has also been found in  $\text{CoCr}_2\text{O}_4$  and  $\text{MnCr}_2\text{O}_4$ ,<sup>7,8</sup> where the presence of a second magnetic cation on the spinel  $A$  site lifts the macroscopic degeneracy. Such non-collinear spiral magnetic order can break spatial inversion symmetry and lead to the appearance of a small electric polarization and pronounced *magneto-electric coupling*.<sup>9,10</sup> Indeed, dielectric anomalies at the magnetic transition temperatures have been found in polycrystalline  $\text{CoCr}_2\text{O}_4$ ,<sup>11</sup> and recently a small electric polarization has been detected in single crystals of the same material.<sup>12</sup> Magnetic spinels therefore constitute a particularly interesting class of frustrated spin systems exhibiting various forms of coupling between their magnetic and structural properties. Furthermore, both  $A$

and  $B$  sites in the spinel structure can be occupied by various magnetic ions and simultaneously the  $X$  anion can be varied between O, S, or Se. This compositional flexibility opens up the possibility to chemically tune the properties of these systems.

To understand the underlying mechanisms of the various forms of magneto-structural coupling, it is important to first understand the complex magnetic structures found in these systems. Such complex magnetic structures can be studied using model Hamiltonians for interacting spin systems, which can be treated either classically or fully quantum mechanically. For the cubic spinel systems, a theory of the ground state spin configuration has been presented by Lyons, Kaplan, Dwight, and Menyuk (LKDM)<sup>13</sup> about 45 years ago. Using a model of classical Heisenberg spins and considering only  $BB$  and  $AB$  nearest neighbor interactions, LKDM could show that in this case the ground state magnetic structure is determined by the parameter

$$u = \frac{4\tilde{J}_{BB}S_B}{3\tilde{J}_{AB}S_A}, \quad (1)$$

which represents the relative strength between the two different nearest neighbor interactions  $\tilde{J}_{BB}$  and  $\tilde{J}_{AB}$ .<sup>14</sup> For  $u \leq u_0 = 8/9$  the collinear Néel configuration, i.e. all  $A$ -site spins parallel to each other and anti-parallel to the  $B$ -site spins, is the stable ground state. For  $u > u_0$  it was shown that a ferrimagnetic spiral configuration has the lowest energy out of a large set of possible spin configurations and that it is locally stable for  $u_0 < u < u'' \approx 1.298$ . For  $u > u''$  this ferrimagnetic spiral configuration is unstable. Therefore, it was suggested that the ferrimagnetic spiral is very likely the ground state for  $u_0 < u < u''$ , but can definitely not be the ground state for  $u > u''$ .<sup>13</sup>

On the other hand it has been found that neutron scattering data for both  $\text{CoCr}_2\text{O}_4$  and  $\text{MnCr}_2\text{O}_4$  are well described by the ferrimagnetic spiral configuration suggested by LKDM, although a fit of the experimental data to the theoretical spin structure leads to values of  $u \approx 2.0$  for  $\text{CoCr}_2\text{O}_4$ ,<sup>8</sup> and  $u \approx 1.6$  for  $\text{MnCr}_2\text{O}_4$ ,<sup>7</sup> which according to the LKDM theory correspond to the locally unsta-

ble regime. Surprisingly, the overall agreement of the fit is better for  $\text{CoCr}_2\text{O}_4$  than for  $\text{MnCr}_2\text{O}_4$ , even though the value of  $u$  for  $\text{CoCr}_2\text{O}_4$  is further within the unstable region than in the case of  $\text{MnCr}_2\text{O}_4$ . From this it has been concluded that: i) the ferrimagnetic spiral is a good approximation of the true ground state structure even for  $u > u''$ , ii) that the importance of effects not included in the theory of LKDM is probably more significant in  $\text{MnCr}_2\text{O}_4$  than in  $\text{CoCr}_2\text{O}_4$ , and iii) that the ferrimagnetic spiral is indeed very likely to be the true ground state for systems with  $u_0 < u < u''$ .<sup>7,8,13</sup>

Recently, Tomiyasu *et al.* fitted their neutron scattering data for  $\text{CoCr}_2\text{O}_4$  and  $\text{MnCr}_2\text{O}_4$  using a ferrimagnetic spiral structure similar to the one proposed by LKDM but with the cone angles of the individual magnetic sublattices not restricted to the LKDM theory.<sup>15</sup> As originally suggested by LKDM, they interpreted their results as indicative of a collinear Néel-like ferrimagnetic component exhibiting long-range order below  $T_C$  and a spiral component, which exhibits only short-range order even in the lowest temperature phase.

In order to assess the validity of the LKDM theory and to facilitate a better comparison with experimental data, an independent determination of the magnetic coupling constants in these systems is very desirable. Density functional theory (DFT, see Ref. 16) provides an efficient way for the *ab initio* determination of such magnetic coupling constants that can then be used for an accurate modeling of the spin structure of a particular system. DFT also offers a straightforward way to investigate the effect of structural distortions on the magnetic coupling constants, and is therefore ideally suited to study the coupling between magnetism and structural properties.

Traditionally, insulating magnetic oxides represent a great challenge for DFT-based methods due to the strong Coulomb interaction between the localized  $d$  electrons. However, recently the local spin density approximation plus Hubbard  $U$  (LSDA+ $U$ ) method has been very successful in correctly determining various properties of such strongly correlated magnetic insulators.<sup>17</sup> In particular, it has been used for the calculation of magnetic coupling constants in a variety of transition metal oxides.<sup>6,18,19,20,21</sup>

Here we present an LSDA+ $U$  study of the magnetic coupling constants in the spinel systems  $\text{CoCr}_2\text{O}_4$  and  $\text{MnCr}_2\text{O}_4$ . The goal of the present paper is to provide accurate values for the relevant coupling constants in these two systems, in order to test the assumptions made by LKDM and to resolve the uncertainties in the interpretation of the experimental data. In addition, we assess the general question of how accurate such magnetic coupling constants in complex oxides can be determined using the LSDA+ $U$  method.

We find that in contrast to the assumptions of the LKDM theory, the coupling between the  $A$  site cations is not necessarily negligible, but that the general validity of the LKDM theory should be better for  $\text{CoCr}_2\text{O}_4$  than for  $\text{MnCr}_2\text{O}_4$ , in agreement with what has been

concluded from the experimental data. However, in contrast to what follows from fitting the experimental data to the LKDM theory, the calculated  $u$  for  $\text{CoCr}_2\text{O}_4$  is smaller than the value of  $u = 2.0$  obtained from the experimental fit. In addition, we show that by analyzing the dependence of the magnetic coupling constants on the LSDA+ $U$  parameters and on the lattice constant, the various mechanisms contributing to the magnetic interaction can be identified, and a quantitative estimate of the corresponding coupling constant can be obtained within certain limits.

The present paper is organized as follows. In Sec. II we present the methods we use for our calculations. In particular, we give a brief overview over the LSDA+ $U$  method and the challenges in using this method as a quantitative and predictive tool. In Sec. III we present our results for the lattice parameters, electronic structure, and magnetic coupling constants of the two investigated Cr spinels. Furthermore, we analyze in detail the dependence of the magnetic coupling constants on the lattice constant and LSDA+ $U$  parameters, and we discuss the reasons for the observed trends. We end with a summary of our main conclusions.

## II. METHODS

### A. LSDA+ $U$

The LSDA+ $U$  method offers an efficient way to calculate the electronic and magnetic properties of complex transition metal oxides. The idea behind the LSDA+ $U$  method is to explicitly include the Coulomb interaction between strongly localized  $d$  or  $f$  electrons in the spirit of a mean-field Hubbard model, whereas the interactions between the less localized  $s$  and  $p$  electrons are treated within the standard local spin density approximation (LSDA).<sup>22</sup> To achieve this, a Hubbard-like interaction term  $E_U$ , which depends on the occupation of the localized orbitals, is added to the LSDA total energy, and an additional double counting correction  $E_{dc}$  is introduced to subtract that part of the electron-electron interaction between the localized orbitals that is already included in the LSDA:

$$E = E_{\text{LSDA}} + E_U - E_{dc} \quad . \quad (2)$$

Here

$$E_U = \frac{1}{2} \sum_{\{\gamma\}} (U_{\gamma_1\gamma_3\gamma_2\gamma_4} - U_{\gamma_1\gamma_3\gamma_4\gamma_2}) n_{\gamma_1\gamma_2} n_{\gamma_3\gamma_4} \quad (3)$$

and

$$E_{dc} = \frac{U}{2} n(n-1) - \frac{\mathcal{J}^H}{2} \sum_s n_s(n_s-1) \quad , \quad (4)$$

where  $\gamma = (m, s)$  is a combined orbital and spin index of the correlated orbitals,  $n_{\gamma_1\gamma_2}$  is the corresponding orbital occupancy matrix,  $n_s = \sum_m n_{ms,ms}$  and

$n = \sum_s n_s$  are the corresponding traces with respect to spin and both spin and orbital degrees of freedom, and  $U_{\gamma_1\gamma_3\gamma_2\gamma_4} = \langle m_1 m_3 | V_{ee} | m_2 m_4 \rangle \delta_{s_1 s_2} \delta_{s_3 s_4}$  are the matrix elements of the screened electron-electron interaction, which are expressed as usual in terms of two parameters, the Hubbard  $U$  and the intra-atomic Hund's rule parameter  $\mathcal{J}^H$  (see Ref. 17).

The LSDA+ $U$  method has been shown to give the correct ground states for many strongly correlated magnetic insulators, and thus represents a significant improvement over the LSDA for such systems.<sup>17</sup> Furthermore, the LSDA+ $U$  method is very attractive due to its simplicity and the negligible additional computational effort compared to a conventional LSDA calculation. It therefore has become a widely used tool for the study of strongly correlated magnetic insulators. Since the LSDA+ $U$  method treats the interactions between the occupied orbitals only in an effective mean-field way, it fails to describe systems where dynamic fluctuations are important. For such systems, the local density approximation plus dynamical mean field theory (LDA+DMFT), which also includes local dynamic correlations, has been introduced recently.<sup>23</sup> However, the LDA+DMFT method is computationally rather demanding, and is currently too costly to be used for the calculation of magnetic characteristics of such complex materials as the spinels. On the other hand, for a large number of systems such fluctuations are of minor importance, and for these systems the LSDA+ $U$  method leads to a good description of the electronic and magnetic properties.

However, in order to obtain reliable results, the use of the LSDA+ $U$  method should be accompanied by a careful analysis of all the uncertainties inherent in this method. An additional goal of the present paper is therefore to critically assess the predictive capabilities of the LSDA+ $U$  method for the determination of magnetic coupling constants in complex transition metal oxides. Apart from the question about the general applicability of the LSDA+ $U$  approach to the investigated system, and the unavoidable ambiguities in the definition of the LSDA+ $U$  energy functional (Eqs. (2)-(4)),<sup>24,25</sup> the proper choice of the parameters  $U$  and  $\mathcal{J}^H$  represents one of the main hurdles when the LSDA+ $U$  method is used as a quantitative and predictive tool.

$U$  and  $\mathcal{J}^H$  can in principle be calculated using constrained density functional theory,<sup>26</sup> thus rendering the LSDA+ $U$  method effectively parameter-free. In practice however, the exact definition of  $U$  and  $\mathcal{J}^H$  within a solid is not obvious, and the calculated values depend on the choice of orbitals or the details of the method used for their determination.<sup>27,28,29,30</sup> Therefore, parameters obtained for a certain choice of orbitals are not necessarily accurate for calculations using a different set of orbitals.

In the present work we thus pursue a different approach. We choose values for  $U$  and  $\mathcal{J}^H$  based on a combination of previous constrained DFT calculations, experimental data, and physical reasoning, and these values are then varied within reasonable limits to study the

resulting effect on the physical properties. In particular, for the spinel systems studied in this work the Hubbard  $U$ s on the transition metal sites are varied between 2 eV and 6 eV (in 1 eV increments), with the additional requirement that  $U_{Cr} \leq U_A$  ( $A = \text{Co, Mn}$ ). For the on-site Hund's rule coupling we use two different values,  $\mathcal{J}^H = 0$  eV and  $\mathcal{J}^H = 1$  eV with  $\mathcal{J}_{Cr}^H = \mathcal{J}_A^H$ . The conditions  $U_{Cr} \leq U_A$  and  $\mathcal{J}_{Cr}^H = \mathcal{J}_A^H$  are motivated by constrained DFT calculations for a series of transition metal perovskite systems, which showed that the Hubbard  $U$  increases continuously from V to Cu, whereas the on-site exchange parameter  $\mathcal{J}^H$  is more or less constant across the series.<sup>28</sup> A similar trend for  $U$  can be observed in the simple transition metal monoxides.<sup>22,29</sup> Although in the spinel structure the coordination and formal charge state of the  $A$  cation is different from the  $B$  cation, we assume that the assumption  $U_{Cr} \leq U_A$  is nevertheless valid, since the screening on the sixfold coordinated  $B$  site is expected to be more effective than on the tetrahedral  $A$  site. Further evidence for the validity of this assumption is given by the relative widths of the  $d$  bands on the  $A$  and  $B$  sites obtained from the calculated orbitally resolved densities of states (see Fig. 1 and Sec. III B).

The absolute values of  $U$  used in this work are motivated by recent constrained DFT calculations using linear response techniques,<sup>29,30</sup> which lead to significantly smaller values of  $U$  than previous calculations using the linear muffin tin orbital (LMTO) method, where the occupation numbers are constrained by simply setting all transfer matrix elements out of the corresponding orbitals to zero.<sup>28,31</sup> Typical values obtained for various transition metal ions in different chemical environments are between 3-6 eV.<sup>29,30</sup> For the  $\text{Cr}^{3+}$  ion a value of  $U \approx 3$  eV, derived by comparing the calculated densities of states with photo-emission data, has been used successfully.<sup>6,32</sup> We thus consider the values  $U_A = 4-5$  eV and  $U_{Cr} = 3$  eV as the most adequate  $U$  parameters for our systems. Nevertheless, we vary these parameters here over a much larger range, in order to see and discuss the resulting trends in the calculated magnetic coupling constants.

For the Hund's rule parameter  $\mathcal{J}^H$  screening effects are less important, and calculated values for various systems are all around or slightly lower than 1 eV.<sup>22,28</sup> On the other hand, a simplified LSDA+ $U$  formalism is sometimes used, where the only effect of  $\mathcal{J}^H$  is to reduce the effective Coulomb interaction  $U_{\text{eff}} = U - \mathcal{J}^H$ .<sup>33,34,35</sup> In this work we use the two values  $\mathcal{J}^H = 0$  eV and  $\mathcal{J}^H = 1$  eV to study the resulting effect on the magnetic coupling constants.

## B. Other technical details

To determine the magnetic coupling constants corresponding to the closest neighbor magnetic interactions between the various sublattices, we calculate the total energy differences for four different collinear magnetic

configurations: the Néel type ferrimagnetic order, the ferromagnetic configuration, and two different configurations with anti-parallel magnetic moments within the  $A$  and  $B$  sub-lattices respectively, and we then project the resulting total energies on a simple classical Heisenberg model,

$$E = - \sum_{i,j} \tilde{J}_{ij} \vec{S}_i \cdot \vec{S}_j = - \sum_{i,j} J_{ij} \hat{e}_i \cdot \hat{e}_j \quad , \quad (5)$$

where only the nearest neighbor coupling constants  $J_{AB}$ ,  $J_{BB}$ , and  $J_{AA}$  are assumed to be nonzero, and where we defined the coupling constants  $J_{ij} = \tilde{J}_{ij} S_i S_j$  corresponding to normalized spin directions  $\hat{e}_i$  of the magnetic ions. We note that even though for itinerant systems such as the elementary magnets Fe, Co, and Ni, the coupling constants obtained in this way can be different from the ones obtained for only small variations from the collinear configurations,<sup>36</sup> the local magnetic moments of many insulating transition metal oxides, in particular the systems investigated in the present study, behave much more like classical Heisenberg spins and thus the simpler approach pursued in this work is justified. We point out that a determination of all possible further neighbor interactions is beyond the scope of this paper and is therefore left for future studies.

We perform calculations at both experimentally determined lattice constants and theoretical lattice parameters. The theoretical lattice parameters are obtained by a full structural relaxation within the LSDA for a collinear Néel-type magnetic configuration. The same LSDA lattice parameters are used in all our calculations with varying values of the LSDA+ $U$  parameters  $U$  and  $\mathcal{J}^H$ . In order to reduce the required computational effort, we do not perform relaxations for each individual set of LSDA+ $U$  parameters. Except when noted otherwise, all calculations are performed using the “Vienna Ab-initio Simulation Package” (VASP) employing the projector augmented wave (PAW) method.<sup>37,38,39</sup> We use a plane wave energy cutoff of 450 eV (550 eV for relaxations) and a  $5 \times 5 \times 5$   $\Gamma$ -centered mesh for Brillouin zone integrations. Increasing the mesh density by using a  $8 \times 8 \times 8$  mesh results only in negligible changes for the calculated total energy differences. Structural relaxations are performed until the forces are less than  $10^{-5}$  eV/Å and all components of the stress tensor are smaller than 0.02 kbar. The electronic self-consistency cycle is iterated until the total energy is converged better than  $10^{-8}$  eV. In addition, we perform some test calculations using the full-potential linear-augmented-plane-wave (FLAPW) method.<sup>40</sup> For these calculations we use the Wien97 code<sup>41</sup> with our own implementation of the LSDA+ $U$  method. The plane-wave cut-off parameter is set to 223 eV in these calculation, and the Brillouin-zone integration is also carried out on a  $5 \times 5 \times 5$   $\Gamma$ -centered mesh. The criterion for self-consistency is the difference in the total energy after the last two iterations being less than  $10^{-4}$  Ry.

TABLE I: Structural parameters calculated in this work.  $a$  is the lattice constant of the cubic spinel structure, and the internal structural parameter  $x$  corresponds to the Wyckoff position 32e ( $x,x,x$ ) of the oxygen sites. Columns “theo.” contain the values calculated in this work while columns “exp.” contain experimental data.

|         | CoCr <sub>2</sub> O <sub>4</sub> |       | MnCr <sub>2</sub> O <sub>4</sub> |       |
|---------|----------------------------------|-------|----------------------------------|-------|
|         | exp. (Ref. 11)                   | theo. | exp. (Ref. 42)                   | theo. |
| $a$ [Å] | 8.335                            | 8.137 | 8.435                            | 8.242 |
| $x$     | 0.264                            | 0.260 | 0.264                            | 0.262 |

### III. RESULTS AND DISCUSSION

#### A. Structural relaxation

Table I shows the structural parameters obtained in this work together with corresponding experimental data. The theoretical lattice constants are obtained within the LSDA and for Néel-type ferrimagnetic order, and are about 2.3 % smaller than the corresponding experimental values for both materials. The calculated internal structural parameters  $x$  are in very good agreement with experiment. The underestimation of the lattice constant by a few percent is a typical feature of the LSDA in complex transition metal oxides.<sup>6,43</sup>

#### B. Electronic structure

Fig. 1 shows the densities of states for both CoCr<sub>2</sub>O<sub>4</sub> and MnCr<sub>2</sub>O<sub>4</sub> calculated using the LSDA and the LSDA+ $U$  method with  $U_A = 5$  eV,  $U_{Cr} = 3$  eV,  $\mathcal{J}_A^H = \mathcal{J}_{Cr}^H = 0$  eV, and a collinear Néel-type magnetic configuration at the experimental lattice constants. Both systems are insulating within the LSDA, although the LSDA energy gap for CoCr<sub>2</sub>O<sub>4</sub> is very small, about 0.15 eV. The LSDA gap is larger for MnCr<sub>2</sub>O<sub>4</sub>, since in this system the gap is determined by the relatively strong crystal-field splitting on the octahedral  $B$  site and the equally strong magnetic splitting, whereas in CoCr<sub>2</sub>O<sub>4</sub> the width of the LSDA gap is limited by the small crystal-field splitting on the tetrahedrally coordinated  $A$  site. The use of the LSDA+ $U$  method increases the width of the energy gap substantially and pushes the majority  $d$  states on the  $A$  site down in energy, leading to strong overlap with the oxygen  $2p$  states. In the LSDA the transition metal  $d$  states are well separated from the oxygen  $p$  manifold, whereas the LSDA+ $U$  method increases the energetic overlap between these states. In all cases the gap is between occupied and unoccupied transition metal  $d$  states.

It can be seen that the bandwidth of the  $d$ -bands for the tetrahedrally coordinated  $A$  site is indeed smaller than for the octahedral  $B$  site. Thus, the  $d$  states on the  $A$  sites are more localized and one can expect a larger on-

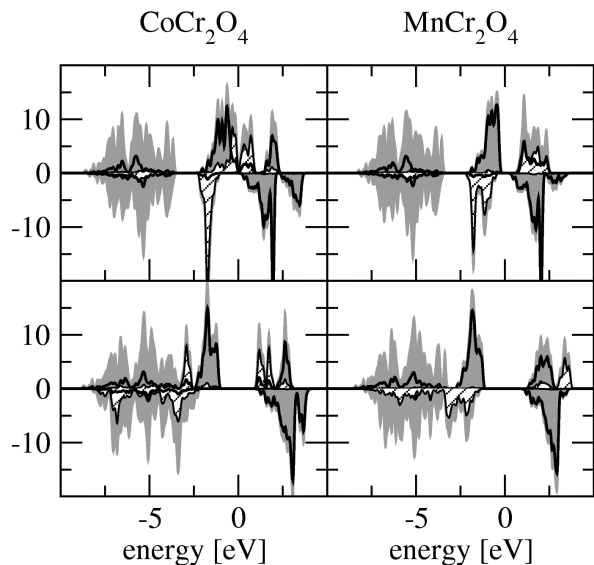


FIG. 1: Densities of states (in states/eV) for  $\text{CoCr}_2\text{O}_4$  (left two panels) and  $\text{MnCr}_2\text{O}_4$  (right two panels) calculated using the LSDA (upper two panels) and the LSDA+ $U$  method with  $U_A = 5\text{ eV}$ ,  $U_{\text{Cr}} = 3\text{ eV}$ , and  $\mathcal{J}_A^H = \mathcal{J}_{\text{Cr}}^H = 0\text{ eV}$  (lower two panels). Calculations were done at the experimental lattice parameters for a collinear Néel-type ferrimagnetic structure where the direction of the Cr magnetic moments was defined as “spin-up”, and corresponding “spin-down” states are shown with a negative sign. The gray shaded areas represent the total density of states, the curves shaded with diagonal lines represent the  $d$  states on the  $A$  site of the spinel lattice, and the thick black lines correspond to the Cr  $d$  states. Zero energy separates the occupied from the unoccupied states.

site Coulomb interaction than on the Cr  $B$  site, in agreement with the assumption that  $U_{\text{Cr}} \leq U_A$  (see Sec. II A).

### C. Magnetic coupling constants

Fig. 2 shows the magnetic coupling constants calculated using the experimental lattice parameters,  $\mathcal{J}_A^H = \mathcal{J}_{\text{Cr}}^H = 1\text{ eV}$ , and different values of the Hubbard  $U$  on the  $A$  and  $B$  sites. All coupling constants are negative, i.e. antiferromagnetic, and decrease in strength when the Hubbard parameters are increased. The “inter-sublattice” coupling  $J_{AB}$  depends similarly on both  $U_A$  and  $U_B$ , whereas both “intra-sublattice” coupling constants  $J_{BB}$  and  $J_{AA}$  depend only on the Hubbard parameter of the corresponding sublattice.

The  $BB$  interaction in the spinel lattice is known to result from a competition between antiferromagnetic (AFM) direct cation-cation exchange and indirect cation-anion-cation exchange, which for the present case of a  $90^\circ$  cation-anion-cation bond angle gives rise to a ferromagnetic (FM) interaction.<sup>44</sup> The AFM direct interaction is expected to dominate at smaller volumes, whereas at larger volumes the FM indirect interaction should be stronger. Furthermore, it is important to note that even

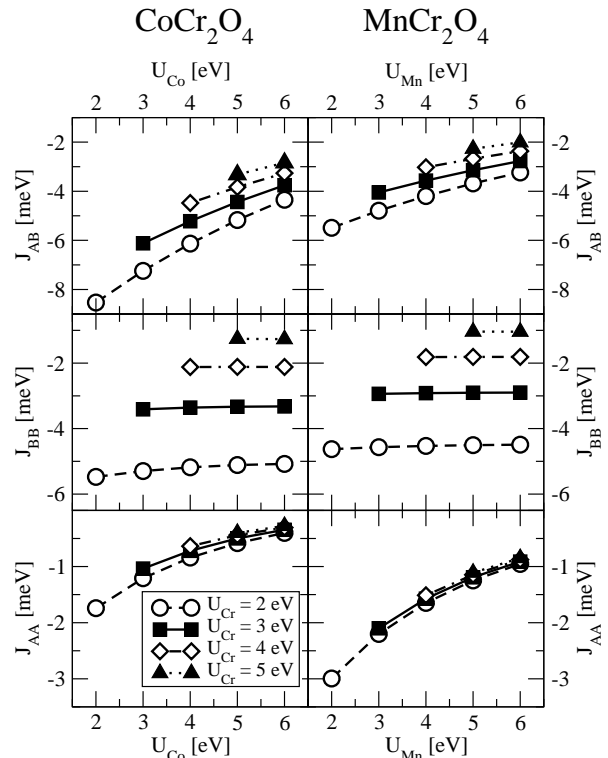


FIG. 2: Magnetic coupling constants  $J_{AB}$  (upper panels),  $J_{BB}$  (middle panels), and  $J_{AA}$  (lower panels) calculated for  $\text{CoCr}_2\text{O}_4$  (left) and  $\text{MnCr}_2\text{O}_4$  (right) as a function of  $U_A$  for  $U_{\text{Cr}} = 2\text{ eV}$  (open circles),  $3\text{ eV}$  (filled squares),  $4\text{ eV}$  (open diamonds), and  $5\text{ eV}$  (filled triangles). All calculations were performed using experimental lattice parameters and  $\mathcal{J}_A^H = \mathcal{J}_{\text{Cr}}^H = 1\text{ eV}$ .

the pure direct cation-cation interaction is comprised out of two parts: (i) the “potential exchange” due to the standard Heitler-London exchange-integral, which is always FM for orthogonal orbitals but is usually negligible, and (ii) the AFM “kinetic exchange”, which results from a second order perturbation treatment of the electron hopping and is proportional to  $1/U$ .<sup>44,45</sup> The observed  $U$  dependence of  $J_{BB}$  can thus be understood as follows: At small values of  $U$  the AFM direct kinetic exchange is strongest, but it is suppressed as the value of  $U$  is increased. The FM indirect cation-anion-cation exchange also decreases, but in addition increasing  $U$  shifts the cation  $d$  states down in energy and thus leads to enhanced hybridization with the anion  $p$  states (see Sec. III B). This enhanced hybridization partially compensates the effect of increasing  $U$  so that the indirect exchange decreases slower than  $1/U$ . Therefore, the FM indirect exchange is less affected by increasing  $U$  than the AFM direct exchange, and thus gains in strength relative to the latter. This explains why the observed decrease of  $J_{BB}$  is stronger than  $1/U$ . In fact, for the larger experimental volumes and using  $J = 0\text{ eV}$  for the Hund’s rule coupling (see discussion below) the  $BB$  coupling in both systems even becomes slightly FM for large  $U$ .

The  $AB$  coupling in the spinels is mediated by a cation-anion-cation bond with an intermediate angle of  $\sim 120^\circ$ , which makes it difficult to predict the sign of the coupling based on general considerations. A weak AFM interaction has been proposed for the case of empty  $e_g$  orbitals on the  $B$  site,<sup>46</sup> in agreement with the present results.

Comparing the values of  $J_{AB}$  and  $J_{BB}$  calculated for a constant set of LSDA+ $U$  parameters shows that both are of the same order of magnitude. On the other hand  $J_{AA}$  is expected to be significantly weaker, since it corresponds to a cation-cation distance of  $\sim 3.6$  Å with the shortest superexchange path along an  $A$ -O-O- $A$  bond sequence. Based on this assumption  $J_{AA}$  was neglected in the theoretical treatment of LKDM.<sup>13</sup> Nevertheless, in our calculations  $J_{AA}$  is found to be of appreciable strength. This is particularly striking for  $\text{MnCr}_2\text{O}_4$ , but also for  $\text{CoCr}_2\text{O}_4$  the difference between  $J_{AA}$  and  $J_{AB}$  ( $J_{BB}$ ) is less than an order of magnitude. From this it follows that  $J_{AA}$  is definitely non-negligible in  $\text{MnCr}_2\text{O}_4$  and can also lead to significant deviations from the LKDM theory in  $\text{CoCr}_2\text{O}_4$ . We point out that this conclusion holds true independently of the precise values of the LSDA+ $U$  parameters used in the calculation. An appreciable value for  $J_{AA}$  has also been found in a previous LSDA study of the spinel ferrite  $\text{MnFe}_2\text{O}_4$ .<sup>47</sup>

As stated in Sec. IIB, a full determination of all possible further neighbor interactions is beyond the scope of this paper. However, to obtain a rough estimate of the strength of further neighbor interactions in  $\text{CoCr}_2\text{O}_4$ , and to see whether this affects the values of  $J_{AB}$ ,  $J_{BB}$ , and  $J_{AA}$  obtained in this work, we perform some additional calculations using a doubled unit cell. This allows us to determine the coupling constant  $J_{BB}^{(3)}$ , corresponding to the third nearest neighbor  $BB$  coupling. As shown in Ref. 48, due to the special geometry of the spinel structure, this third nearest neighbor coupling is larger than all other further neighbor interactions within the  $B$  sublattice, and can be expected to represent the next strongest magnetic interaction apart from  $J_{BB}$ ,  $J_{AB}$ , and  $J_{AA}$ . This coupling is mediated by a  $B$ -O-O- $B$  bond sequence and corresponds to a  $BB$  distance of 5.89 Å. For comparison, the distances corresponding to  $J_{BB}$ ,  $J_{AB}$ , and  $J_{AA}$  are 2.94 Å, 3.46 Å, and 3.61 Å, respectively.<sup>49</sup> For these test calculations we use the experimental lattice parameters of  $\text{CoCr}_2\text{O}_4$  and the LSDA+ $U$  parameters  $U_{\text{Co}} = 5$  eV,  $U_{\text{Cr}} = 3$  eV, and  $\mathcal{J}^H = 0$  eV. We obtain a value of  $J_{BB}^{(3)} = 0.15$  eV, corresponding to a weak FM coupling. However, the magnitude of  $J_{BB}^{(3)}$  is small compared to  $J_{AB}$  and  $J_{BB}$ , and we therefore continue to neglect further neighbor interactions in the following.

Next we calculate the magnetic coupling constants using the lattice parameters obtained by a full structural optimization within the LSDA, and also by using  $\mathcal{J}^H = 0$  eV at both experimental and theoretical lattice parameters. Again, we vary  $U_A$  and  $U_{\text{Cr}}$  independently. The observed variation of the coupling constants with respect to the Hubbard parameters is very similar to the

TABLE II: Calculated magnetic coupling constants  $J_{AB}$ ,  $J_{BB}$ , and  $J_{AA}$  for different lattice parameters and different values of the intra-atomic Hund’s rule coupling parameter  $\mathcal{J}^H$  for  $U_A = 5$  eV and  $U_{\text{Cr}} = 3$  eV. Lattice parameters “exp.” and “theo.” refer to the corresponding values listed in Table I.

| $\mathcal{J}^H$ (eV)      |                | 1.0   | 0.0   | 1.0   | 0.0   |
|---------------------------|----------------|-------|-------|-------|-------|
| latt. param.              |                | exp.  | exp.  | theo. | theo. |
| $\text{CoCr}_2\text{O}_4$ | $J_{AB}$ (meV) | -4.44 | -3.55 | -6.02 | -4.83 |
|                           | $J_{BB}$ (meV) | -3.33 | -1.04 | -6.90 | -4.34 |
|                           | $J_{AA}$ (meV) | -0.50 | -0.44 | -0.77 | -0.58 |
| $\text{MnCr}_2\text{O}_4$ | $J_{AB}$ (meV) | -3.14 | -1.40 | -4.88 | -2.61 |
|                           | $J_{BB}$ (meV) | -2.91 | -0.74 | -5.22 | -2.74 |
|                           | $J_{AA}$ (meV) | -1.19 | -0.92 | -1.88 | -1.45 |

case shown in Fig. 2, only the overall magnitude of the magnetic coupling constants is changed. We therefore discuss only the results obtained for  $U_{\text{Cr}} = 3$  eV and  $U_A = 5$  eV, which are physically reasonable choices for these parameters, as discussed in Sec. IIA.

Table II shows the calculated magnetic coupling constants for the different cases. It is apparent that both volume and the intra-atomic exchange parameter  $\mathcal{J}^H$  have a significant effect on the calculated results. The volume dependence can easily be understood. The smaller theoretical volume leads to stronger coupling between the magnetic ions. This is particularly significant for  $J_{BB}$ , since the direct exchange interaction between the  $B$  cations is especially sensitive to the inter-cation distance. The corresponding coupling is therefore strongly enhanced (suppressed) by decreasing (increasing) the lattice constant. The indirect superexchange interaction also depends strongly on the inter-atomic distances.

It can be seen from Table II that  $\mathcal{J}^H = 0$  significantly decreases the strength of all magnetic coupling constants compared to  $\mathcal{J}^H = 1$  eV. A strong  $\mathcal{J}^H$  dependence of the magnetic coupling has also been observed in other Cr spinels with non-magnetic cations on the  $A$  site.<sup>50</sup> Further calculations, with different values for  $\mathcal{J}^H$  on the  $A$  and  $B$  sites respectively, show that it is mostly  $\mathcal{J}_{\text{Cr}}^H$  which is responsible for this effect. On the other hand, varying  $\mathcal{J}_A^H$  has a smaller effect on the magnetic coupling. This is consistent with the very strong  $\mathcal{J}^H$  dependence of  $J_{BB}$  and the weaker  $\mathcal{J}^H$  dependence of  $J_{AA}$  seen in Table II.

To understand the strong effect of  $\mathcal{J}_{\text{Cr}}^H$  on the magnetic coupling constants we first take a look at the occupation numbers  $n_\gamma \equiv n_{\gamma\gamma}$  of the Cr  $d$  orbitals. The corresponding occupation numbers in  $\text{CoCr}_2\text{O}_4$  are (calculated for a FM configuration at the experimental lattice parameters and using  $\mathcal{J}^H = 0$ ):  $n_{t_{2g},\uparrow} = 0.95$ ,  $n_{t_{2g},\downarrow} = 0.05$ ,  $n_{e_g,\uparrow} = 0.32$ , and  $n_{e_g,\downarrow} = 0.21$ . As expected, the occupation of the  $t_{2g}$  orbitals represents the formal  $d^3$  valency with full spin-polarization, but in addition there is a sizable  $e_g$  occupation, which contributes  $\sim 0.2\mu_B$  to the local spin moment of the Cr cation. This partial  $e_g$

occupation, which is due to hybridization with the oxygen  $p$  bands, gives rise to a FM interaction between the Cr sites, because the  $e_g$  polarization is coupled to the  $t_{2g}$  spins via the Hund's rule coupling.<sup>44</sup> This FM interaction between the Cr sites should therefore be proportional to the strength of the Hund's rule coupling. Thus, the stronger AFM interaction for  $\mathcal{J}^H = 1$  eV compared to  $\mathcal{J}^H = 0$  (see Table II) might be surprising at first. However, it is important to realize that even though the parameter  $\mathcal{J}^H$  represents the strength of the Hund's rule coupling, its effect within the LSDA+ $U$  framework is not to introduce a strong Hund's rule interaction. If one analyzes the LSDA+ $U$  energy expression, Eq. (2), in a somewhat simplified picture where the occupation matrix is diagonal and the Coulomb matrix elements are orbitally independent, one can see that the double counting correction,  $E_{dc}$ , exactly cancels the different potential shifts for orbitals with parallel and antiparallel spins that are caused by  $E_U$  for  $\mathcal{J}^H \neq 0$ , if one of the  $d$  orbitals is filled. Thus,  $E_U - E_{dc}$  does not lead to an additional Hund's rule interaction compared to  $E_{LSDA}$ , even for  $\mathcal{J}^H \neq 0$ . It is generally assumed that this type of interaction is already well described on the LSDA level. The only effect of  $\mathcal{J}^H$  is therefore an effective reduction of the on-site Coulomb repulsion. This can be seen in the following, where we write the simplified version of Eq. (2) as (see Ref. 33):

$$E = E_{LSDA} + \frac{U_{\text{eff}}}{2} \left( n - \sum_{\gamma} n_{\gamma} n_{\gamma} \right), \quad (6)$$

with  $U_{\text{eff}} = U - \mathcal{J}^H$ . Within this simplified LSDA+ $U$  version, the effect of  $\mathcal{J}^H$  on the magnetic coupling constant can be understood as an effective reduction of the on-site Coulomb interaction. According to the previously discussed  $U$  dependence of the magnetic coupling constants (see also Fig. 2), a reduced on-site Coulomb interaction leads to a stronger AFM interaction for all calculated magnetic coupling constants.

From Fig. 2 it can be seen that the magnetic coupling constants for  $\text{CoCrO}_2$  using experimental lattice parameters and the LSDA+ $U$  parameters  $U_{\text{Co}} = 6$  eV,  $U_{\text{Cr}} = 4$  eV, and  $\mathcal{J}^H = 1$  eV, i.e.  $U_{\text{eff,Co}} = 5$  eV and  $U_{\text{eff,Cr}} = 3$  eV, are:  $J_{AB} = -3.26$  eV,  $J_{BB} = -2.12$  eV, and  $J_{AA} = -0.30$  eV. The corresponding result for  $U_{\text{Co}} = 5$  eV,  $U_{\text{Cr}} = 3$  eV, and  $\mathcal{J}^H = 0$ , i.e. for the same values of  $U_{\text{eff}}$  but different  $\mathcal{J}^H$ , are:  $J_{AB} = -3.55$  eV,  $J_{BB} = -1.04$  eV, and  $J_{AA} = -0.44$  eV (see Table II). Thus, the pure dependence on  $U_{\text{eff}}$  seems to be approximately valid for  $J_{AB}$  and  $J_{AA}$ , whereas there is a notable quantitative deviation from the simplified LSDA+ $U$  model in the case of  $J_{BB}$ . Nevertheless, the overall trend can still be understood from the simplified LSDA+ $U$  picture.

Finally, to assess the possible influence of different methods to solve the self-consistent Kohn-Sham equations on the calculated magnetic coupling constants, we perform additional tests using a different electronic structure code employing the FLAPW method (see Sec. II B).

TABLE III: Magnetic coupling constants of  $\text{CoCr}_2\text{O}_4$  and  $\text{MnCr}_2\text{O}_4$  calculated using two different methods (FLAPW and PAW), different values for  $\mathcal{J}^H$ , and the experimental lattice parameters.

|                           | $\mathcal{J}^H$ (eV) | FLAPW |       | PAW   |       |
|---------------------------|----------------------|-------|-------|-------|-------|
|                           |                      | 0.0   | 1.0   | 0.0   | 1.0   |
| $\text{CoCr}_2\text{O}_4$ | $J_{AB}$ (meV)       | -3.62 | -4.32 | -3.55 | -4.44 |
|                           | $J_{BB}$ (meV)       | -1.32 | -3.09 | -1.04 | -3.33 |
|                           | $J_{AA}$ (meV)       | -0.23 | -0.00 | -0.44 | -0.50 |
| $\text{MnCr}_2\text{O}_4$ | $J_{AB}$ (meV)       | -1.73 | -3.23 | -1.40 | -3.14 |
|                           | $J_{BB}$ (meV)       | -1.32 | -3.21 | -0.74 | -2.91 |
|                           | $J_{AA}$ (meV)       | -0.67 | -1.06 | -0.92 | -1.19 |

The results are summarized and compared to the PAW results in Table III. There are some variations in the absolute values of the magnetic coupling constants obtained with the two different methods, but overall the agreement is rather good. Trends are the same in both methods, and in particular the strong effect of the LSDA+ $U$  Hund's rule parameter  $\mathcal{J}^H$  on the magnetic coupling constants is confirmed by the FLAPW calculations. One possible reason for the differences between the PAW results and the FLAPW results is that the radii of the projection spheres used in the PAW method are chosen differently from the radii of the Muffin-Tin spheres used to construct the FLAPW basis functions.

#### D. The LKDM parameter $u$

Figure 3 shows the variation of the LKDM parameter  $u = \frac{4J_{BB}S_B}{3J_{AB}S_A} = \frac{4J_{BB}}{3J_{AB}}$  with the strength of the on-site Coulomb interactions for the different lattice parameters and values of  $\mathcal{J}^H$  used in this work. The behavior of  $u$  follows from the corresponding trends in the coupling constants  $J_{AB}$  and  $J_{BB}$  discussed in the previous section. Increasing  $U_A$  decreases the strength of  $J_{AB}$  but leaves  $J_{BB}$  more or less unchanged, and thus increases the value of  $u$ . On the other hand both  $J_{AB}$  and  $J_{BB}$  decrease with increasing  $U_{\text{Cr}}$ , but the decrease is stronger for  $J_{BB}$  and therefore  $u$  decreases with increasing  $U_{\text{Cr}}$ . Thus, the trends caused by the Hubbard parameters corresponding to the two different magnetic sites are opposite to each other.

As already pointed out in the previous section, changing the value of the LSDA+ $U$  parameter  $\mathcal{J}^H$  and using different lattice constants essentially just shifts the overall scale for the magnetic coupling constants without altering their  $U$  dependence. Therefore, using the larger experimental volume decreases  $u$  compared to the value obtained at the theoretical lattice parameters due to the very strong volume dependence of  $J_{BB}$ . Introducing the on-site Hund's rule coupling  $\mathcal{J}^H$  increases  $u$ , since  $J_{BB}$  is stronger affected by this and thus increases relative to

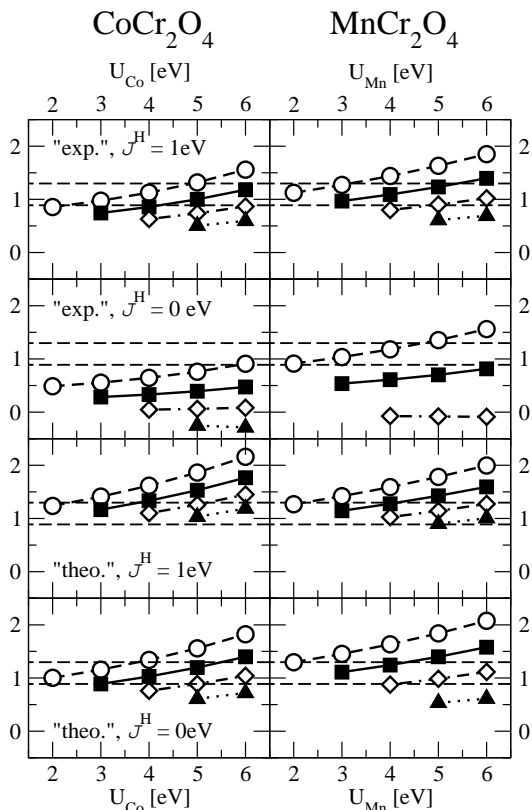


FIG. 3: Dependence of the LKDM parameter  $u$  on the Hubbard  $U$  parameters of the different magnetic cations. Left panels correspond to  $\text{CoCr}_2\text{O}_4$ , right panels to  $\text{MnCr}_2\text{O}_4$ . From top to bottom the different panels correspond to calculations for exp. volume and  $\mathcal{J}^H = 1$  eV, exp. volume and  $\mathcal{J}^H = 0$  eV, theo. volume and  $\mathcal{J}^H = 1$  eV, and theo. volume and  $\mathcal{J}^H = 0$  eV (open circles:  $U_{\text{Cr}} = 2$  eV, filled squares:  $U_{\text{Cr}} = 3$  eV, open diamonds:  $U_{\text{Cr}} = 4$  eV, filled triangles:  $U_{\text{Cr}} = 5$  eV). Dashed horizontal lines indicate the critical values  $u_0 = 8/9$  and  $u'' \approx 1.298$ .

### $J_{AB}$ .

For similar values of  $U_A$  and  $U_{\text{Cr}}$  the LKDM parameter  $u$  is larger in  $\text{MnCr}_2\text{O}_4$  than in  $\text{CoCr}_2\text{O}_4$ , except for  $\mathcal{J}^H = 1$  eV at the theoretical lattice parameters, where they are approximately equal. This is in contrast to what has been concluded by fitting the experimental neutron spectra to the spiral spin structure of the LKDM theory, which leads to the values  $u=1.6$  for  $\text{MnCr}_2\text{O}_4$  and  $u=2.0$  for  $\text{CoCr}_2\text{O}_4$ ,<sup>7,8</sup> i.e. the fitted value for  $\text{CoCr}_2\text{O}_4$  is significantly larger than the value for  $\text{MnCr}_2\text{O}_4$ .

We now try to give a quantitative estimate of  $u$  in the two systems. The first question is whether using experimental or theoretical lattice constants leads to more realistic magnetic coupling constants. This question is not easy to answer in general. On the one hand, the LSDA underestimation of the lattice constant can lead to an overestimation of the magnetic coupling, since the cations are too close together and can therefore interact stronger than at the experimental volume. On the other hand, the indirect cation-anion-cation interaction

is intimately connected to the chemical bonding.<sup>44</sup> If the larger experimental lattice constant is used, this bonding is artificially suppressed and the corresponding magnetic coupling is eventually underestimated. It is therefore not obvious whether it is better to calculate the coupling constants at the experimental or the theoretical lattice parameters, but the two cases at least provide reasonable limits for the magnetic coupling constants. We note that using the LSDA+ $U$  method for the structural relaxation, usually leads to lattice parameters that are in slightly better agreement with the experimental values,<sup>43</sup> which will decrease the corresponding uncertainty in the magnetic coupling constants. In the present paper we do not perform such structural relaxations for each combination of the LSDA+ $U$  parameters, in order to reduce the required computational effort. In addition, this allows us to discuss the pure effect of  $U$  and  $\mathcal{J}^H$  on the magnetic coupling constants, without contributions due to varying lattice parameters.

Fig. 3 shows that for the physically reasonable parameters  $U_{\text{Cr}} = 3$  eV,  $U_A = 4-5$  eV, and  $\mathcal{J}^H = 1$  eV the value of  $u$  in  $\text{CoCr}_2\text{O}_4$  calculated at the theoretical lattice constant is slightly larger than the critical value  $u'' \approx 1.298$ , where within the LKDM theory the ferrimagnetic spiral configuration becomes unstable. In  $\text{MnCr}_2\text{O}_4$  the corresponding value is about equal to  $u''$ . At the experimental lattice constants the values of  $u$  in both systems are smaller than at the theoretical lattice constants, with the stronger effect in  $\text{CoCr}_2\text{O}_4$ , where  $u$  at the theoretical lattice constant is about equal to  $u_0 = 8/9$ , the value below which, according to LKDM, a collinear ferrimagnetic spin configuration is the ground state. In  $\text{MnCr}_2\text{O}_4$  the value of  $u$  at the experimental lattice constant is between  $u_0$  and  $u''$ . Thus, in all cases the calculated values of  $u$  are consistent with the experimental evidence for noncollinear ordering.

Since in  $\text{MnCr}_2\text{O}_4$  the calculation predicts a rather strong  $J_{AA}$ , the validity of the LKDM theory is questionable for this system, but for  $\text{CoCr}_2\text{O}_4$ , where the magnitude of  $J_{AA}$  is indeed significantly smaller than both  $J_{AB}$  and  $J_{BB}$ , this theory should at least be approximately correct. However, for  $\text{CoCr}_2\text{O}_4$  the calculated  $u$  both at experimental and at the theoretical lattice constant (and using physically reasonable values for the LSDA+ $U$  parameters) is still significantly smaller than the value  $u = 2.0$  obtained by fitting the experimental data to the LKDM theory.<sup>8</sup> It would therefore be interesting to study how the incorporation of  $J_{AA}$  into a generalized LKDM theory alters the conclusions drawn from the experimental data. Obviously, a non-negligible  $J_{AA}$  will further destabilize the collinear Néel configuration, but the possible influence of  $J_{AA}$  on the ferrimagnetic spiral structure cannot be obtained straightforwardly. Of course it cannot be fully excluded that the discrepancy between the calculated value of  $u$  for  $\text{CoCr}_2\text{O}_4$  and the value extracted from the experimental data is caused by some deficiencies of the LSDA+ $U$  method. For example, it was shown in Ref. 18 that for  $\text{MnO}$  the LSDA+ $U$



method does not offer enough degrees of freedom to correctly reproduce both nearest and next nearest neighbor magnetic coupling constants.

Finally, we note that the fact that  $J_{AA}$  is not negligible in  $\text{MnCr}_2\text{O}_4$  but has a significantly smaller magnitude than  $J_{AB}$  and  $J_{BB}$  in  $\text{CoCr}_2\text{O}_4$  is compatible with the fact that the overall agreement between the experimental data and the LKDM theory is better for  $\text{CoCr}_2\text{O}_4$  than for  $\text{MnCr}_2\text{O}_4$ .<sup>8</sup> However, a quantitative discrepancy between the value of  $u$  for  $\text{CoCr}_2\text{O}_4$  calculated in this work and the value derived from the experimental data remains.

#### IV. SUMMARY AND CONCLUSIONS

In summary, we have presented a detailed LSDA+ $U$  study of magnetic coupling constants in the spinel systems  $\text{CoCr}_2\text{O}_4$  and  $\text{MnCr}_2\text{O}_4$ . We have found that the coupling between the  $A$  site cations, which is neglected in the classical theory of LKDM, is of appreciable size in  $\text{CoCr}_2\text{O}_4$  and definitely not negligible in  $\text{MnCr}_2\text{O}_4$ . The calculated LKDM parameter  $u$ , which describes the relative strength of the  $BB$  coupling compared to the  $AB$  coupling and determines the nature of the ground state spin configuration in the LKDM theory, is found to be smaller than the values obtained by fitting experimental neutron data to the predictions of the LKDM theory. It remains to be seen whether this discrepancy is caused by the simplifications made in the LKDM theory, or whether

it is due to deficiencies of the LSDA+ $U$  method used in our calculations.

In addition, we have shown that it is difficult, but possible, to arrive at quantitative predictions of magnetic coupling constants using the LSDA+ $U$  method. In addition, by analyzing the  $U$  and  $\mathcal{J}^H$  dependence of the magnetic coupling constants it is possible to identify the various interaction mechanisms contributing to the overall magnetic coupling. The presence of two different magnetic cations with different charge states and different anion coordination, promotes the systems investigated in this work to a very hard test case for the predictive capabilities of the LSDA+ $U$  method. Nevertheless, some insight can be gained by a careful analysis of all methodological uncertainties, and the magnitudes of the magnetic coupling constants can be determined to a degree of accuracy that allows to establish important trends and predict the correct order of magnitude for the corresponding effects.

#### Acknowledgments

C.E. thanks Craig Fennie, Ram Seshadri, Nicola Spaldin, and Andrew Millis for useful discussions. This work was supported by the NSF's *Chemical Bonding Centers* program, Grant No. CHE-0434567 and by the MRSEC Program of the NSF under the award number DMR-0213574. We also made use of central facilities provided by NSF-MRSEC Award No. DMR-0520415.

---

\* Electronic address: ederer@phys.columbia.edu

<sup>1</sup> A. P. Ramirez, in *Handbook of magnetic materials*, edited by K. H. J. Bushow (Elsevier Science B. V., 2001), vol. 13, chap. 4.  
<sup>2</sup> A. P. Ramirez, *Nature (London)* **421**, 483 (2003).  
<sup>3</sup> S.-H. Lee, C. Broholm, T. H. Kim, W. Ratcliff II, and S.-W. Cheong, *Phys. Rev. Lett.* **84**, 3718 (2000).  
<sup>4</sup> J.-H. Chung, M. Matsuda, S.-H. Lee, K. Kakurai, H. Ueda, T. J. Sato, H. Takagi, K.-P. Hong, and S. Park, *Phys. Rev. Lett.* **95**, 247204 (2005).  
<sup>5</sup> A. B. Sushkov, O. Tchernyshyov, W. Ratcliff II, S. W. Cheong, and H. D. Drew, *Phys. Rev. Lett.* **94**, 137202 (2005).  
<sup>6</sup> C. J. Fennie and K. M. Rabe, *Phys. Rev. Lett.* **96**, 205505 (2006).  
<sup>7</sup> J. M. Hastings and L. M. Corliss, *Phys. Rev.* **126**, 556 (1962).  
<sup>8</sup> N. Menyuk, K. Dwight, and A. Wold, *J. Phys. (Paris)* **25**, 528 (1964).  
<sup>9</sup> T. Kimura, T. Goto, H. Shintani, K. Ishizaka, T. Arima, and Y. Tokura, *Nature (London)* **426**, 55 (2003).  
<sup>10</sup> G. Lawes, A. B. Harris, T. Kimura, N. Rogado, R. J. Cava, A. Aharony, O. Entin-Wohlmann, T. Yildirim, M. Kenzelmann, C. Broholm, et al., *Phys. Rev. Lett.* **95**, 087205 (2005).  
<sup>11</sup> G. Lawes, B. Melot, K. Page, C. Ederer, M. A. Hayward, T. Proffen, and R. Seshadri, *Phys. Rev. B* **74**, 024413

(2006).

<sup>12</sup> Y. Yamasaki, S. Miyasaka, Y. Kaneko, J.-P. He, T. Arima, and Y. Tokura, *Phys. Rev. Lett.* **96**, 207204 (2006).  
<sup>13</sup> D. H. Lyons, T. A. Kaplan, K. Dwight, and N. Menyuk, *Phys. Rev.* **126**, 540 (1962).  
<sup>14</sup> In this nomenclature the Heisenberg interaction energy is expressed as  $E_{ij} = -2\tilde{J}_{ij}\vec{S}_i \cdot \vec{S}_j$ , where  $\vec{S}_i$  is a classical vector of length  $S_i$ , the total spin of ion  $i$ .  
<sup>15</sup> K. Tomiyasu, J. Fukunaga, and H. Suzuki, *Phys. Rev. B* **70**, 214434 (2004).  
<sup>16</sup> R. O. Jones and O. Gunnarsson, *Rev. Mod. Phys.* **61**, 689 (1989).  
<sup>17</sup> V. I. Anisimov, F. Aryasetiawan, and A. I. Liechtenstein, *J. Phys.: Condens. Matter* **9**, 767 (1997).  
<sup>18</sup> I. V. Solov'yev and K. Terakura, *Phys. Rev. B* **58**, 15496 (1998).  
<sup>19</sup> A. N. Yaresko, V. N. Antonov, H. Eschrig, P. Thalmaier, and P. Fulde, *Phys. Rev. B* **62**, 15538 (2000).  
<sup>20</sup> P. Baettig, C. Ederer, and N. A. Spaldin, *Phys. Rev. B* **72**, 214105 (2005).  
<sup>21</sup> P. Novák and J. Ruzs, *Phys. Rev. B* **71**, 184433 (2005).  
<sup>22</sup> V. I. Anisimov, J. Zaanen, and O. K. Andersen, *Phys. Rev. B* **44**, 943 (1991).  
<sup>23</sup> V. I. Anisimov, A. I. Potaryayev, M. A. Korotin, A. O. Anokhin, and G. Kotliar, *J. Phys.: Condens. Matter* **9**, 7359 (1997).  
<sup>24</sup> I. V. Solov'yev, P. H. Dederichs, and V. I. Anisimov, *Phys.*

- Rev. B **50**, 16861 (1994).
- <sup>25</sup> M. T. Czyżyk and G. A. Sawatzky, Phys. Rev. B **49**, 14211 (1994).
- <sup>26</sup> P. H. Dederichs, S. Blügel, R. Zeller, and H. Akai, Phys. Rev. Lett. **53**, 2512 (1984).
- <sup>27</sup> M. S. Hybertsen, M. Schlüter, and N. E. Christensen, Phys. Rev. B **39**, 9028 (1989).
- <sup>28</sup> I. Solovyev, N. Hamada, and K. Terakura, Phys. Rev. B **53**, 7158 (1996).
- <sup>29</sup> W. E. Pickett, S. C. Erwin, and E. C. Ethridge, Phys. Rev. B **58**, 1201 (1998).
- <sup>30</sup> M. Cococcioni and S. de Gironcoli, Phys. Rev. B **71**, 035105 (2005).
- <sup>31</sup> V. I. Anisimov and O. Gunnarsson, Phys. Rev. B **43**, 7570 (1991).
- <sup>32</sup> C. J. Fennie and K. M. Rabe, Phys. Rev. B **72**, 214123 (2005).
- <sup>33</sup> H. Sawada, Y. Morikawa, K. Terakura, and N. Hamada, Phys. Rev. B **56**, 12154 (1997).
- <sup>34</sup> S. L. Dudarev, G. A. Botton, S. Y. Savrasov, C. J. Humphreys, and A. P. Sutton, Phys. Rev. B **57**, 1505 (1998).
- <sup>35</sup> C. Ederer and N. A. Spaldin, Phys. Rev. B **71**, 224103 (2005).
- <sup>36</sup> A. I. Liechtenstein, M. I. Katsnelson, and V. A. Gubanov, J. Phys. F: Met. Phys. **14**, L125 (1984).
- <sup>37</sup> P. E. Blöchl, Phys. Rev. B **50**, 17953 (1994).
- <sup>38</sup> G. Kresse and J. Furthmüller, Phys. Rev. B **54**, 11169 (1996).
- <sup>39</sup> G. Kresse and D. Joubert, Phys. Rev. B **59**, 1758 (1999).
- <sup>40</sup> E. Wimmer, H. Krakauer, M. Weinert, and A. J. Freeman, Phys. Rev. B **24**, 864 (1981).
- <sup>41</sup> P. Blaha, K. Schwarz, P. Sorantin, and S. B. Trickey, Comput. Phys. Commun. **59**, 399 (1990).
- <sup>42</sup> R. Seshadri, private communication.
- <sup>43</sup> J. B. Neaton, C. Ederer, U. V. Waghmare, N. A. Spaldin, and K. M. Rabe, Phys. Rev. B **71**, 014113 (2005).
- <sup>44</sup> J. B. Goodenough, *Magnetism and the Chemical Bond* (Interscience Publishers, New York, 1963).
- <sup>45</sup> P. W. Anderson, in *Magnetism*, edited by G. T. Rado and H. Suhl (Academic Press, 1963), vol. 1, chap. 2, pp. 25–83.
- <sup>46</sup> D. G. Wickham and J. B. Goodenough, Phys. Rev. **115**, 1156 (1959).
- <sup>47</sup> D. J. Singh, M. Gupta, and R. Gupta, Phys. Rev. B **65**, 064432 (2002).
- <sup>48</sup> K. Dwight and N. Menyuk, Phys. Rev. **163**, 435 (1967).
- <sup>49</sup> All values refer to  $\text{CoCr}_2\text{O}_4$  and experimental lattice parameters.
- <sup>50</sup> C. J. Fennie, in preparation.